![MolecularLibraries - Pathways to Discovery]

Probe Report

Title: Small Molecule Inhibitors of the Human Apurinic/apyrimidinic Endonuclease 1 (APE1)

Authors: Ganesha Rai[a], Vaddadi N. Vyjayanti [b], Dorjbal Dorjsuren[a], Anton Simeonov[a], Ajit Jadhav[a], David M. Wilson[b], David J. Maloney[a*]

[a] NIH Chemical Genomics Center, National Human Genome Research Institute, National Institutes of Health, Rockville, Maryland.

[b] National Institute on Aging, National Institutes of Health, Bethesda, Maryland.

* To whom correspondence should be addressed: NIH Chemical Genomics Center, NIH Center for Translational Therapeutics, National Human Genome Research Institute, National Institutes of Health, 9800 Medical Center Drive, Building B, Bethesda, MD 20892-3370. Phone: 301-217-4381. Fax: 301-217-5736. Email: maloneyd@mail.nih.gov

Assigned Assay Grant #: MH086444
Screening Center Name & PI: NIH Chemical Genomics Center, Christopher P. Austin
Chemistry Center Name & PI: NIH Chemical Genomics Center, Christopher P. Austin
Assay Submitter & Institution: David M. Wilson III, NIH, National Institute on Aging
**PubChem Summary Bioassay Identifier (AID):** 2324

Abstract:

Probe compound, ML199, and related inhibitors of Apurinic/apyrimidinic (AP) endonuclease (APE1) are reported herein. APE1 is a key component of the base excision repair (BER) pathway that is responsible for repair of DNA damage caused by many anti-cancer agents such as bleomycin and temozolomide. As a result, inhibition of APE1 has been postulated as a viable strategy for sensitizing tumor cells to chemotherapy. ML199 and its related analogs belong to a drug-like series that was identified and optimized through a focused medicinal chemistry effort to afford compounds which display competitive inhibition of APE1 activity in the low micromolar potency range. On target effect of the ML199 was demonstrated through a concentration depended inhibition of AP site incision activity in whole cell HeLa extracts.

Moreover, ML199 potentiated the cytotoxicity of the DNA alkylating agent methylmethane sulfonate (MMS) at non-cytotoxic doses of the probe compound. The probe and its general class of compounds have shown to have good kinetic solubility, Caco-2 permeability, metabolic stability and other favorable physicochemical properties, thus making ML199 an ideal starting point for further pre-clinical development of anti-cancer agents.

Probe Structure & Characteristics:
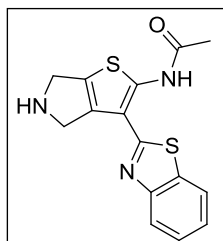
ML199

CID/ML#	Target Name	IC$_{50}$/EC$_{50}$ (nM) [SID, AID]	Anti-target Name(s)	IC$_{50}$/EC$_{50}$ (μM) [SID, AID]	Fold Selective	Secondary Assay(s) Name: IC$_{50}$/EC$_{50}$ (nM) [SID, AID]
CID 46925884/ ML199	APE1	6000 nM IC$_{50}$ [SID 99430950, AID 2572]	Thiazole orange counterscreen	> 57 μM IC$_{50}$ [SID 99430950, AID 2741]	> 10 fold	RIA gel assay: 1000 nM IC$_{50}$ [SID 99430950, AID 488940]

Recommendations for scientific use of the probe:

The novel optimized probe described in this report (ML199) can be used for target validation of APE1 in enzymatic and cell-based systems. It can also be used in combination with known DNA cancer chemotherapeutics, such as temozolomide (TMZ), to potentiate the activity of these agents. It can be utilized in studies involving the BER pathway and the potentiation of known cancer chemotherapeutics. Lastly, the general class of this probe and its analogs has good *in vitro* ADME properties, making the probe series useful in further optimization for potential *in vivo* exposure.
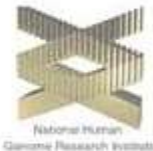
1   Introduction

The goal of this project is to develop chemical probes directed at the human BER enzyme, APE1. Such probes will enhance our understanding of the role of APE1 in normal and cancer cells and may provide opportunities for developing novel anticancer agents that potentiate genotoxic treatments. BER is the major pathway for dealing with spontaneous hydrolytic, oxidative and alkylative base and sugar damage to DNA[1]. Central to this process is incision at an apurinic/apyrimidinic (AP) site that is generated either spontaneously or via the enzymatic activity of a DNA repair glycosylase. This strand cleavage step is performed by the main, if not sole, mammalian AP endonuclease, APE1[2;3]. APE1 has been found to be essential for not only animal viability, as deletion of both alleles of the APE1 gene in mice leads to embryonic lethality[4], but also for cell viability in culture[5;6]. Moreover, past studies incorporating either antisense or RNAi strategies have revealed that APE1-deficient cells exhibit hypersensitivity to a number of "DNA-damaging" agents, including the laboratory chemicals methyl methanesulfonate (MMS), hydrogen peroxide, menadione and paraquat, and the anticancer agents ionizing radiation, thiotepa, 1,3-bis(2-chloroethyl)-1-nitrosourea (a.k.a. Carmustine), TMZ, gemcitabine, and the nucleoside analog ß-L-dioxolane-cytidine (a.k.a. Troxacitabine)[7]. Recent work from the Wilson group employing a dominant-negative APE1 protein (termed ED), which binds with high affinity to substrate DNA and blocks subsequent repair steps[8], has shown that ED augments the cell killing of 5-fluorouracil (~fivefold) and 5-fluorodeoxyuridine (~thirtyfold), implicating BER in the cellular response to such antimetabolites as well. These data underscore the potential of APE1 as an inhibitor target in the effort to improve therapeutic efficacy of clinical DNA-interactive drugs through inactivation of DNA repair responses[9].

Most drugs employed to eradicate neoplastic disease (e.g. alkylators, cross-linking agents, intercalating agents, topoisomerase inhibitors, DNA cleaving agents and certain antimetabolites) operate by inducing the formation of complex DNA lesions/intermediates that ultimately block

replication of rapidly dividing cells, such as cancer cells, and activate cell death responses. A primary goal of current studies is to devise combinatorial methods that (a) protect normal cells from the toxic effects of anti-cancer agents and (b) enhance the sensitivity of tumor cells. As alluded to above, DNA repair systems represent a major protective mechanism against the cytotoxic effects of clinical DNA-interactive compounds. Thus, recent efforts have focused on the design of novel small molecule inhibitors of specific DNA repair proteins, for instance, the DNA strand break response protein poly(ADP)ribose polymerase PARP1[10].

Whereas extensive studies have been performed using various genetic and molecular techniques to delineate the cellular effects of a BER deficiency, experiments employing inhibitor molecules are comparatively lacking and would complement existing knowledge and potentially provide novel biological insights. Moreover, recent evidence has implicated BER capacity as an important factor in determining individual responsiveness to clinical DNA-interactive agents, most notably alkylators (e.g. TMZ) and antimetabolites (e.g. 5-fluorouracil and certain nucleoside analogs) used in the treatment of cancer, and in some instances, viral infections[11]. Alkylators induce cell killing through the formation of alkylated bases, many of which are either lost spontaneously to form abasic sites or are substrates for DNA glycosylases[12]; TMZ is a promising drug recently added to the arsenal of alkylating agents for the adjuvant chemotherapy of brain cancers due to its ability to readily cross the blood-brain barrier[13]. The antimetabolite 5-fluorouracil, which has been used clinically for ~40 years and is commonly employed in the eradication of colorectal and pancreatic cancers, induces cell death by promoting the introduction of uracil and fluorouracil bases into DNA, which are ultimately processed by BER glycosylases[14,15]. All told, BER inhibitors or activators would provide novel resources that may improve efficacy of current treatment paradigms by promoting selective sensitization or protection of diseased and normal cells, respectively. *In vitro* inhibitors of APE1 identified within are prospective reagents for the design of high affinity compounds with potential therapeutic value in combinational treatments.

Prior Art:

Compound **1**[16] (see **Table 1**) was the first reported direct APE1 AP endonuclease inhibitor and is currently sold by Sigma-Aldrich chemical company; however, several groups have failed to reproduce the APE1 inhibitory activity of this compound. In agreement with these findings, our group was also unable to reproduce the activity in both the HTS and radiotracer incision assays. Arylstilbonic acid **2** displays potent activity against APE1 with a submicromolar IC_{50} (low micromolar in our assay); however, this class of compounds has limited efficacy in cellular assays due to poor cellular uptake[17]. Zawahir *et al*. described the utilization of a pharmacophore model to identify compounds such as **3**, which display low μM inhibition against APE1 incision activity. However, given the presence of three carboxylic acid moieties in many of their described inhibitors, it is unlikely that these compounds will have acceptable cell permeability[18]. Additionally, this report contained limited biochemical data using a purified enzyme assay; thus, the compounds' utility as APE1 probes is unknown.

Most recently, Kelley and co-workers[19] described the HTS of 60,000 small molecules and found several low micromolar hits against APE1. The most promising was compound **4**, which had a reported IC_{50} of 2.1 μM in whole cell extract AP endonuclease assays and inhibited the repair of AP sites in SF767 glioblastoma cells. Moreover, AR03 was reported to potentiate the cytotoxicity of the alkylators methyl methansulfonate (MMS) and TMZ in SF767 cells. This compound is actually a part of the MLSMR library (MLS000552981) and had weak activity in our assay, ~31 μM. While the reason for this discrepancy is not fully understood, it may likely be due to the differences in AP endonuclease conditions used in the respective studies. Nevertheless, these studies provide us a direct comparison of our probe compound with previously reported APE1 inhibitors.

During the course of our assay development and LOPAC screening, we identified aurintricarboxylic acid (ATA, a stable radical polymer), 6-hydroxy-DL DOPA, Tyrphostin AG 538, myricetin, thiolactomycin, and mitoxantrone as inhibitors of APE1 AP site incision activity[20] (*see* **Figure 1**). These compounds have been noted to affect multiple targets, including numerous DNA-processing enzymes. In addition to their known promiscuous nature, none of the compounds represented a good starting point for extensive optimization.
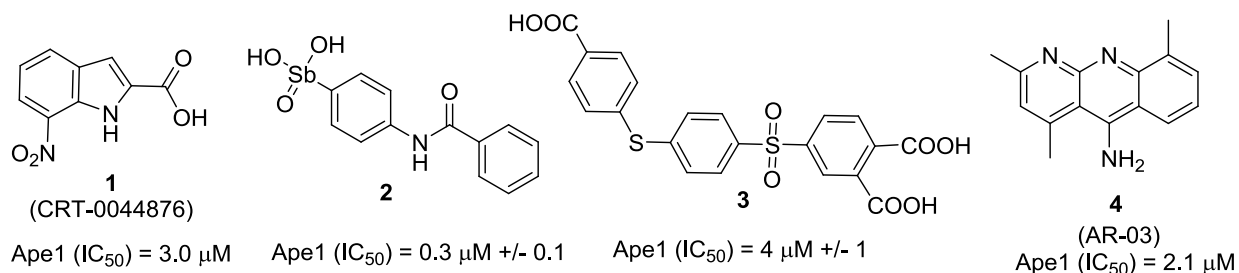
Figure 1. Hit compounds identified from the LOPAC screen.

2   Materials and Methods

General Methods for Chemistry. Unless otherwise stated, all reactions were carried out under an atmosphere of dry argon or nitrogen in dried glassware. Indicated reaction temperatures refer to those of the reaction bath, while room temperature (rt) is noted as 25 ^{o}C. All solvents were of anhydrous quality, purchased from Aldrich Chemical Co. and used as received. Commercially available starting materials and reagents were purchased from Aldrich and were used as received. Analytical thin layer chromatography (TLC) was performed with Sigma Aldrich TLC plates (5 x 20 cm, 60 Å, 250 µm). Visualization was accomplished by irradiation under a 254 nm UV lamp. Chromatography on silica gel was performed using forced flow (liquid) of the indicated solvent system on Biotage KP-Sil pre-packed cartridges and the Biotage SP-1 automated chromatography system. ^{1}H- and ^{13}C NMR spectra were recorded on a Varian Inova 400 MHz spectrometer. Chemical shifts are reported in ppm with the solvent resonance as the internal standard (CDCl$_3$ 7.26 ppm, 77.00 ppm, DMSO-d_6 2.49 ppm, 39.51 ppm for ^{1}H, ^{13}C respectively). Data are reported as follows: chemical shift, multiplicity (s = singlet, d = doublet, t = triplet, q = quartet, br = broad, m = multiplet), coupling constants, and number of protons. Low resolution mass spectra (electrospray ionization) were acquired on an Agilent Technologies 6130 quadrupole spectrometer coupled to the HPLC system. High resolution mass spectral data were collected in-house using an Agilent 6210 time-of-flight mass spectrometer, also coupled to an Agilent Technologies 1200 series HPLC system. If needed, products were purified via a Waters semi-preparative HPLC equipped with a Phenomenex Luna$^{®}$ C18 reverse phase (5 micron, 30 x 75 mm) column having a flow rate of 45 mL/min. The mobile phase was a mixture of acetonitrile (0.025% TFA) and H$_2$O (0.05% TFA), and the temperature was maintained at 50 ^{o}C.

Samples were analyzed for purity on an Agilent 1200 series LC/MS equipped with a Luna® C18 reverse phase (3 micron, 3 x 75 mm) column having a flow rate of 0.8-1.0 mL/min over a 7-minute gradient and an 8.5 minute run time. Purity of final compounds was determined to be >95%, using a 3 µL injection with quantitation by AUC at 220 and 254 nm (Agilent Diode Array Detector).

2.1   Assays

APE1 qHTS Assay: Inhibition of APE1 activity was screened (AID 2517) by utilizing double-stranded short substrate containing a tetrahydrofuran (THF) abasic site labeled with rhodamine-type fluorophore (TAMRA) at the 5'-end and with non-fluorescent Black Hole Quencher-2 (BHQ-2) at the opposing 3'-end. An increase in the fluorescence intensity due to incision of the abasic site by APE1 was used to measure the enzyme activity. Three µL of enzyme were dispensed to 1536-well Greiner black solid bottom plates. Compounds (23 nL) were transferred via Kalypsys pintool. The plates were incubated for 15 min at room temperature, and then 1 µL of substrate solution was added to start the reaction. The plates were immediately transferred into a ViewLux High-throughput CCD imager (Perkin-Elmer) in order to measure the reaction progress in kinetic mode (three reads every 60 seconds) using a 525 nm excitation and 598 nm emission fluorescence protocol. The fluorescence intensity difference between the third and the first time points was used to compute reaction progress. Reagents and Controls: Substrate: 50 nM final concentration of TAMRA/BHQ-2 substrate dispensed throughout the plate. Enzyme: 0.75 nM APE1 final concentration in columns 1, 2, 5-48. Column 1 is neutral (100% activity). Control: Pintool transfer of control inhibitor NSC-13755 to column 2 of all assay plates. Two-fold, 16-pt dilution in duplicate to produce final concentrations in the 5.75 µM - 0.175 nM range. Buffer columns in columns 3 and 4 were used as negative control (no enzyme).

Thiazole Orange Assay for Promiscuous DNA Binding: In order to distinguish true inhibitors of DNA-processing enzymes from promiscuous DNA-binding compounds among screening assay hits, we developed a homogeneous and miniaturized assay (AID 2741) based on fluorescent dye displacement test as originally described by Tse and Boger[21]. The assay is based on the strong enhancement of fluorescence when Thiazole Orange (ThO) binds to double-stranded DNA; conversely, in the presence of a DNA-binding compound, Thiazole Orange is

displaced from the DNA and its fluorescence is reduced. Three μL of reaction buffer (50 mM Tris-HCl pH7.5, 50 mM NaCl, 2 mM MgCl2, 1 mM DTT and 0.01% Tween-20) containing 250 nM ThO and 50 nM dsDNA (upper strand 5' TC ACC FTC GTA CGA CTC, lower strand 3' AG TGG GAG CAT GCT GAG, F denotes tetrahydrofuran) were dispensed into a 1536-well Greiner black assay plate via solenoid-valve based nanoliter dispensers. Compounds (23 nL each in columns 5-48) and control (23 nL each in column 2 as dose-response) were transferred via a Kalypsys pintool equipped with a 1536-pin array. The plates were incubated for 15 min at room temperature and were then transferred into a ViewLux high-throughput CCD imager, where the endpoint fluorescence was measured using a 480 nm excitation and 540 nm emission protocol.

Radiotracer Incision Assay (RIA). Recombinant wild type APE1 protein was purified as previously described[22]. Fifty pg of APE1 (~140 pM) was incubated without (positive control containing 1% DMSO) or with 100 μM of the indicated inhibitor at room temperature in RIA buffer (50 mM Tris pH 7.5, 25 mM NaCl, 1 mM $MgCl_2$, 1 mM DTT, 0.01% Tween -20) for 15 min. One-half pmol of ^{32}P 5'-radiolabeled AP-DNA substrate (18 mer) was added to a 10 μL final volume[23], and the reactions were incubated at 37 ^{o}C for 5 min and stopped by adding stop buffer (0.05% Bromophenol blue/ Xylene cyanol dissolved in 95% formamide, 20 mM EDTA) and heating at 95 ^{o}C for 10 min. Intact substrate was separated from incised product on a 15% polyacrylamide denaturing gel in tris boric acid EDTA buffer. Following electrophoresis, the gel was subjected to standard phosphoimager analysis using the ImageQuant 5.2 software, and the percent incision activity (amount of substrate converted to product) was calculated. For IC_{50} determinations (i.e. the concentration of inhibitor at which 50% inactivation was observed), 50 pg of APE1 (~140 pM) was incubated without or with increasing concentrations (1 nM to 100 μM) of the indicated inhibitor as above, and the percent incision activity was determined. IC_{50}s were extrapolated from duplicate experimental sets after plotting the results using GraphPad Prism 4.0. PubChem AID 488940.

Electrophoretic Mobility Shift Assay (EMSA). Three hundred ng of APE1 (~0.8 μM) was incubated without inhibitor (positive control, 1% DMSO) or with increasing concentrations of inhibitor (1, 3, 10, 30 pr 100 μM) in binding buffer (50 mM Tris pH 7.5, 25 mM NaCl, 1 mM EDTA, 1 mM DTT, 10% glycerol, 0.01% Tween 20) for 10 min on ice, and then radiolabeled ^{32}P

AP-DNA substrate (100 fmol) was added to a 10 μL final volume. Following incubation on ice for 5 min, samples were subjected to non-denaturing polyacrylamide gel electrophoresis (20 mM Tris pH 7.5, 10 mM sodium acetate, 0.5 mM EDTA, 8% polyacrylamide, 2.5% glycerol) for 2 hr at 120 V in electrophoresis buffer (20 mM Tris pH 7.5, 10 mM sodium acetate, 0.5 mM EDTA) to separate the APE1-DNA complex from unbound radiolabeled DNA[24]. After electrophoresis, the gel was subjected to standard phosphoimager analysis as above, and the percentage of substrate DNA in complex with APE1 was determined.

HeLa Whole Cell Extract Incision Assay. HeLa cells maintained in DMEM with 10% fetal bovine serum and 1% Penicillin-Streptomycin were harvested, washed with 1X PBS, and re-suspended in hypotonic ice cold lysis buffer (50 mM Tris pH 7.4, 1 mM EDTA, 1 mM DTT, 10% glycerol, 0.5 mM PMSF). The suspension was frozen at -80 ^{o}C for at least 30 min and then slowly thawed at 4 ℃ for ~1 hr. KCl was then added to the cell suspension to a final concentration of 222 mM, followed by incubation on ice for 30 min and clarification by centrifugation at 12,000 xg for 15 min at 4 ℃. The supernatant (whole cell extract) was retained, the protein concentration determined using the Bio-Rad Bradford reagent, and aliquots stored until needed at -80 ℃. Three hundred ng of HeLa whole cell extract was incubated with 0, 50 or 100 μM of the indicated inhibitor at room temperature for 15 min prior to the addition of 0.5 pmol of ^{32}P radiolabeled AP-DNA substrate (final volume of 10 μL). The reaction mix was then transferred to 37 ℃ for 5 min to allow for incision. Following addition of stop buffer and heat denaturation, the reaction products were analyzed as above.

MMS Potentiation Cell-based Assay. HeLa cells were plated by multichannel pipette or Multidrop Combi dispenser (Thermo) at 6K/25 μL/well in DMEM culture medium, plus 10% FBS, into white solid bottom 384-well cell culture plates. The plates were incubated at 37 ℃ overnight for cell attachment. The following day, the cell medium in each well was replaced with fresh medium containing MMS (0.4 mM final concentration) and/or serial dilutions of compounds of interest, except for the vehicle controls. The plates were incubated for 24 hr at 37 ℃. Cell viability was evaluated by adding 15 μL of CellTiter Glo reagent (Promega, Madison, WI) and incubating the plate at room temperature for 30 min, and subsequently measuring the luminescence in ViewLux reader. Percent viability was calculated for each concentration of tested compounds in duplicates, relating the luminescence to the negative DMSO control. MMS

potentiation trends were defined as follows: (-), if cell viability was the same as that of the DMSO control; (+), if the cell viability decrease was between 20-40%; and (++), if the cell viability decrease was more than 40% in presence of test compounds.

2.2   Probe Chemical Characterization
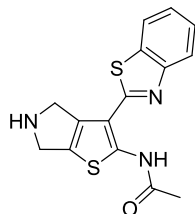
Probe Characterization (ML199):

***Purity >95% as judged by LC/MS and ^{1}H NMR**

***N*-(3-(benzo[d]thiazol-2-yl)-5,6-dihydro-4H-thieno[2,3-c]pyrrol-2-yl)acetamide**: LC-MS: rt (min) = 3.98; ^{1}H NMR (400 MHz, DMSO-d_6) δ 2.36 (s, 3 H), 4.54 (s, 2 H), 4.68 (s, 2 H), 7.49 (t, *J* = 7.6 Hz, 1 H), 7.61 (t, *J* = 7.7 Hz, 1 H), 8.17 (t, *J* = 7.5 Hz, 2 H), 9.94 (brs, 1 H), and 12.03 (brs, 1 H); HRMS (ESI) *m/z* (M+Na)$^+$ calcd. for $C_{15}H_{13}N_3OS_2Na$, 338.0403; found 338.0403.

LC/MS conditions:

- LC/MS (Agilent system) Retention time t_1 (short) = **2.88** min and t_2 (long) = **3.88**.
- Column: 3 x 75 mm Luna C18, 3 micron
- Run time: 4.5 min (short); 8.5 min (long)
- Gradient: 4 % to 100 %
- Mobile phase: Acetonitrile (0.025 % TFA), water (0.05 % TFA)
- Flow rate: 0.8 to 1.0 mL
- Temperature: 50°C
- UV wavelength: 220 nm, 254 nm

MLSMR Numbers for Probe and Analogs:

MLS ID	NCGC ID	SID	CID	ML	Type
MLS003178551	NCGC00185090	SID 99430950	CID 46925884	ML199	Probe
MLS003178552	NCGC00184830	SID 99430935	CID 4055306		Analog
MLS003178553	NCGC00184832	SID 99430937	CID 46925888		Analog
MLS003178554	NCGC00184834	SID 99430938	CID 46925885		Analog
MLS003178555	NCGC00185094	SID 99430953	CID 46925861		Analog
MLS003178556	NCGC00186101	SID 99430962	CID 46925887		Analog

Probe *in vitro* ADME properties:

- Aqueous (kinetic) solubility in PBS buffer (pH 7.4 @ 25 ^{o}C): 51.6 μM
- Caco-2 permeability (P_{app} x 10^6)/cm-s^{-1}: 6.8
- Efflux ratio (B→A)/(A→B): 0.81
- hERG inhibition-Qpatch-whole-cell patch clamp (IC$_{50}$): 8.04 μM (note original "hit" was 0.66 μM)
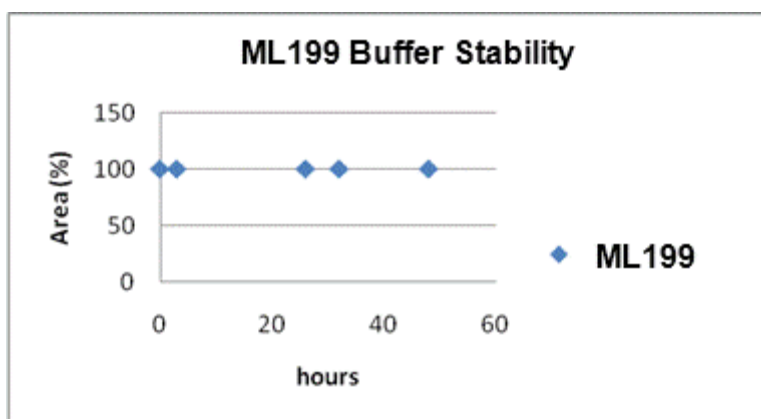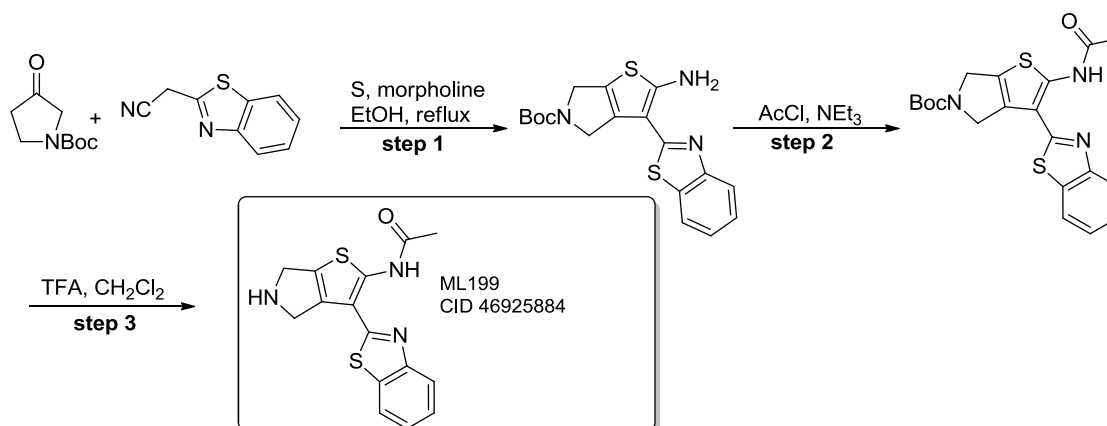- mouse plasma stability (T ½) = >120 min

Figure 2. Buffer Stability (48 hrs @ 25 ^{o}C) of ML199.

Scheme 1. Synthetic route to ML199.

2.3 Probe Preparation

The synthesis commenced using the Gewald's 2-aminothiophene reaction[25] of commercially available *t*-butyl-3-oxopyrrolidine-1-carboxylate in the presence of sulfur and morpholine to afford the fused product[26] (see **Scheme 1**). The regiochemistry of the formed product was determined by NMR spectroscopy. Acetylation of the 2-amino group was achieved with acetyl choride in the presence of triethyl amine, and subsequent Boc-deprotection with TFA gave the probe molecule in good yield.

Preparation of *t*-butyl 2-amino-3-(benzo[d]thiazol-2-yl)-4H-thieno[3,2-c]pyrrole-5(6H)-carboxylate (Step 1): A mixture of *t*-butyl 3-oxopyrrolidine-1-carboxylate (1.0 g, 5.4 mmol, 1 eq.), 2-(benzo[d]thiazol-2-yl)acetonitrile (0.94 g, 5.4 mmol, 1 eq.), sulfur (0.17 g, 5.4 mmol, 1 eq.) and morpholine (0.47 mL, 5.4 mmol, 1 eq.) in ethanol (25 mL) was refluxed for 1 hr. Excess solvent was removed under diminished pressure and the crude product was recrystallized from ethanol. Yield: 1.6 g (79%).

Preparation of *t*-butyl 2-acetamido-3-(benzo[d]thiazol-2-yl)-4H-thieno[3,2-c]pyrrole-5(6H)-carboxylate (Step 2): To a mixture of *t*-butyl 2-amino-3-(benzo[d]thiazol-2-yl)-4H-thieno[3,2-c]pyrrole-5(6H)-carboxylate (1.0 g, 2.7 mmol, 1 eq.) and triethylamine (1.1 mL, 8.0 mmol, 3 eq.) in dichloromethane (25 mL) was added acetyl chloride (0.29 mL, 4.0 mmol, 1.5 eq.) dropwise at 0 °C. The reaction mixture was stirred at room temperature for 2 hrs, then diluted with dichloromethane, and the organic layer was successively with water, saturated bicarbonate solution and brine. The organic layer was dried on sodium sulfate and evaporated to afford the crude solid which was further purified on a Biotage® silica gel column. Gradient elution with 2% methanol in dichloromethane gave the product. Yield: 0.99 g (89%).

Preparation of *N*-(3-(benzo[d]thiazol-2-yl)-5,6-dihydro-4H-thieno[3,2-c]pyrrol-2-yl)acetamide (step 3): *t*-Butyl 2-acetamido-3-(benzo[d]thiazol-2-yl)-4H-thieno[3,2-c]pyrrole-5(6H)-carboxylate (0.5 g, 1.59 mmol) in dichloromethane (10 mL) was added with TFA (5 mL) and was stirred at room temperature for 1 h. The volatiles were removed under reduced pressure and the crude product was purified in a preparative HPLC (see general methods for details) to afford the pure product.

General Procedure for reductive amination (for analogs containing substitution on piperidine nitrogen): Sodium cyanoborohydride (3 mmol, 3 eq.) and few drops of acetic acid were added to a mixture of appropriate amine (1 mmol, 1 eq.) and acetone/appropriate carbonyl compound (10 mmol, 10 eq.) in a mixture of MeOH/THF (0.2 molar reaction concentration). The reaction mixture was stirred at room temperature for 6-10 h. Volatiles were removed and the crude solid was purified on a preparative HPLC.

3   Results

3.1   Summary of Screening Results

A robust modified donor/quencher-based assay was further miniaturized into a 1536-well format and used to identify small molecule inhibitors of APE1. Briefly, a deoxyoligonucleotide containing a tetrahydrofuran (THF) abasic-site analog labeled on the 5'-end with 6-TAMRA was annealed to its complementary strand, where the 3'-end was labeled with a Black Hole Quencher-2 (BHQ2), to create an artificial DNA substrate for the APE1 enzyme. Upon cleavage of the abasic site by APE1, a short deoxyoligonucleotide product labeled with TAMRA was spontaneously released from the remaining DNA, causing the fluorophore emission to increase by up to 10-fold under the assay conditions. Prior to the full-collection screen, the assay was tested and found to perform reproducibly by screening the LOPAC[1280] (library of pharmacologically active compounds) in triplicate using a fully-integrated robotic system. The assay was then applied to screen a 239,513-compound library arrayed as seven-point titrations ranging from 57 μM to 2.9 nM. In total, 1,339 assay plates, containing 2,056,704 wells, were screened in one continuous robotic run lasting approximately 84 hrs. Overall, the assay performed well during the entire course of the screen: intra-plate control titration (NSC 13755) was stable, with an average IC_{50} of 0.035 μM and a minimum significant ratio of 1.9; the Z' factor remained consistent without fluctuations, at an average of 0.79.

In contrast to traditional HTS, qHTS provides a concentration response curve (CRC) for each compound and allows for calculation of an AC_{50} value (defined as the half-maximal activity concentration) for each compound in the primary screen. In this screen, the inhibition associated with each well was computed from the alteration in fluorescence intensity over the time-course measurement period, normalized against control wells. Analysis of the qHTS results revealed

that the top filtered samples (based on curve quality and potency) led to 121 clusters and 154 singletons, consisting of approximately 1,100 compounds with full concentration-response curves and IC_{50} values of less than 30 µM. Results can be seen in **Figure 3**. To define the structure activity relationship (SAR) between the various compounds that elicited inhibition of APE1 activity, we clustered the structures showing high and low quality CRC by structural similarity. This enabled us to find a series of inhibitors with a common core and to query the entire qHTS dataset to identify those related structures associated with a weaker CRC or inactivity. This approach allows determination of a complete SAR from the qHTS to be developed for novel lead compounds. After exclusion of strong auto-fluorescent compounds, compounds active in the thiazole orange dye displacement DNA binding assay, antimony-containing compounds, and various mercury and other heavy-metal-containing molecules, 471 compounds remained. These were tested in a radiotracer assay for orthogonal confirmation, resulting in the identification of the present chemotype (*see* **Figure 4**). The initial active for probe chemotype is CID 3581333 (MLS000419194, resynthesized as NCGC00183664-01).

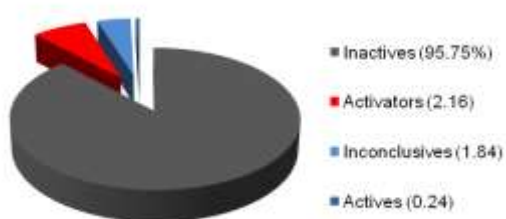**A) APE1 qHTS Activity Plot**
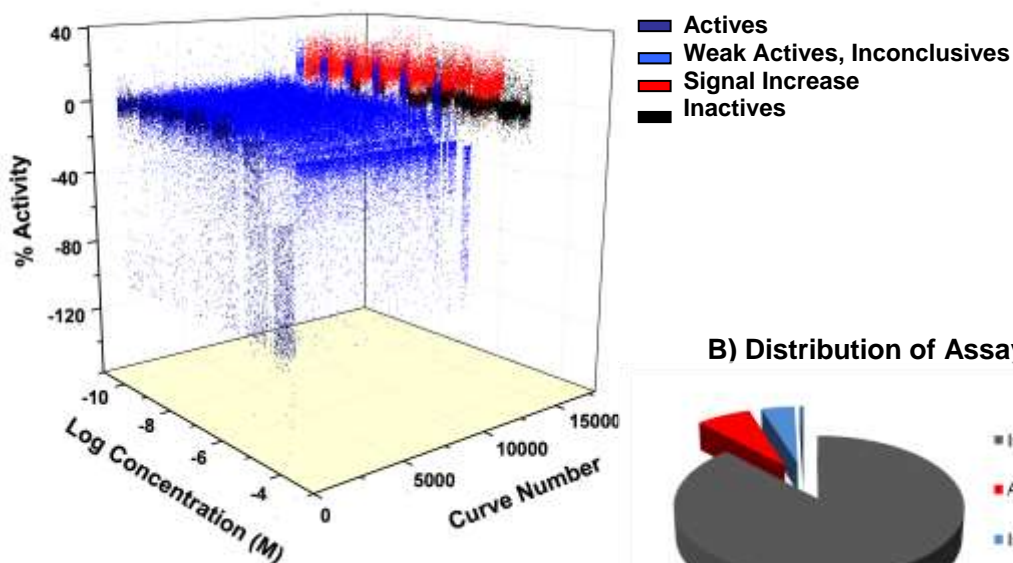
Figure 3. Activity from the primary qHTS screen (A) and distribution of the assay response against the chemical library (B).
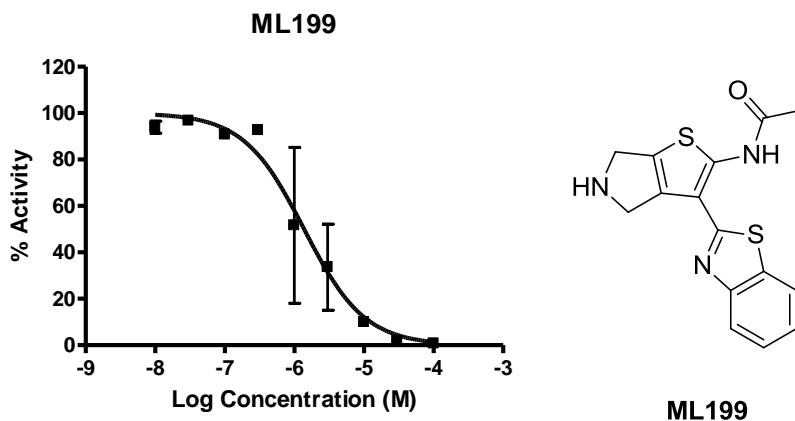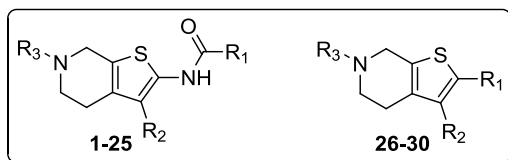
3.2   Dose Response Curves for Probe

ML199

Figure 4. Dose response from ML199 in Radiotracer Incision Assay and structure of the probe.

## 3.3   Scaffold/Moiety Chemical Liabilities

While many of the series found in the qHTS contained reactive functional groups, the series chosen for probe development did not contain any serious liabilities.

3.4 SAR Tables

Entry	CID	SID	NCGC IDs	R₁	R₂	R₃	HTS potency (μM) [RIA IC50 (μM)], n= replicates
1	3581333	99430932	NCGC00183664-01	Me	benzothiazole	$CH(CH_3)_2$	10 [19], n = 2
2	46925879	99430934	NCGC00184829-01	Me	benzothiazole	H	6 [5], n = 2
3	46925863	99430933	NCGC00184828-01	Me	benzothiazole	Boc	31 [ND], n = 2
4	4055306	99430935	NCGC00184830-01	Me	benzothiazole	Me	6 [5], n = 2
5	4532325	99430936	NCGC00184831-01	Me	benzothiazole	Bn	18 [ND], n = 2
6	4348310	99430945	NCGC00185083-01	Me	benzothiazole	Ac	10 [5], n = 2
7	46925878	99430951	NCGC00185091-01	Me	H	H	>56 [ND], n = 2
8	46925860	99430960	NCGC00186096-01	Me	2-furan	H	18 [ND], n = 2
9	46925883	99430961	NCGC00186097-01	Me	2-thiophene	H	36 [ND], n = 2
10	46925887	99430962	NCGC00186101-01	Me	2-benzofuran	H	18 [ND], n = 2
11	46925876	99430963	NCGC00187565-01	Me	2-indole	H	>56 [ND], n = 2
12	46925880	99430964	NCGC00187566-01	Me	2-thiazole	H	23 [ND], n = 2
13	46925872	99430959	NCGC00186075-01	Me	Ph	H	>56 [ND], n = 2
14	46925888	99430937	NCGC00184832-01	Me	benzoxazole	$CH(CH_3)_2$	23 [13], n = 2
15	46925885	99430938	NCGC00184834-01	Me	2-(4-phenylthiazole)	$CH(CH_3)_2$	6 [3], n = 2
16	4138521	99430940	NCGC00184838-01	$C(CH_3)_3$	benzothiazole	$CH(CH_3)_2$	25 [ND], n = 2
17	4053204	99430941	NCGC00184839-01	cyclopropane	benzothiazole	$CH(CH_3)_2$	18 [ND], n = 2
18	43950654	99430942	NCGC00184840-01	cyclopentane	benzothiazole	$CH(CH_3)_2$	11 [ND], n = 2
19	4107484	99430939	NCGC00184837-01	Ph	benzothiazole	$CH(CH_3)_2$	16 [ND], n = 2
20	46925867	99430944	NCGC00185082-01	CF_3	benzothiazole	H	31 [ND], n = 2
21	46925862	99430967	NCGC00189087-01	OMe	benzothiazole	H	6 [ND], n = 2
22	46925861	99430953	NCGC00185094-01	CHF_2	benzothiazole	H	3 [4], n = 2
23	46925869	99430946	NCGC00185085-01	$(CH_2)_2C\equiv CH$	benzothiazole	H	14 [ND], n = 2
24	46925865	99430947	NCGC00185086-01	$(CH_2)_2C\equiv CH$	benzothiazole	$CH(CH_3)_2$	11 [ND], n = 2
25	46925871	99430966	NCGC00189084-01	(image)	benzothiazole	H	>56 [ND], n = 2
26	46925873	99430965	NCGC00189083-01	(image)	benzothiazole	H	23 [ND], n = 2
27	46925877	99430969	NCGC00189234-01	(image)	benzothiazole	H	16 [ND], n = 2
28	46925868	99430968	NCGC00189233-01	(image)	benzothiazole	H	16 [ND], n = 2
29	46925866	46925866	NCGC00184843-01	NH_2	benzothiazole	$CH(CH_3)_2$	41 [ND], n = 2

Table 1. SAR Table - APE1 inhibition: representative analogs. Note: all compounds in table were synthesized at NCGC. ND = not determined.
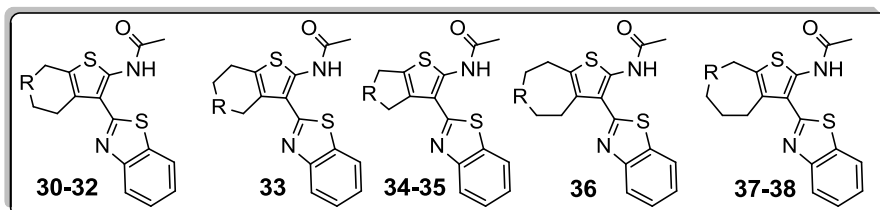
Entry	CID	SID	NCGC IDs	R	HTS potency (μM) [RIA IC50 (μM)], n= replicates
30	46925881	99430948	NCGC00185087-01	O	18 [ND], n = 2
31	46925864	99430949	NCGC00185089-01	S	16 [ND], n = 2
32	46925882	99430955	NCGC00185096-01	$S(O)_2$	11* [77], n = 2
33	46925874	99430954	NCGC00185095-01	NH	45 [ND], n = 2
34	46925884	99430950	NCGC00185090-01	NH	6 [1], n = 2
35	46925875	99430952	NCGC00185093-01	$N(CH(CH_3)_2$	3 [4], n = 2
36	46925870	99430958	NCGC00185100-01	$N(CH(CH_3)_2$	18 [13], n = 2
37	46925889	99430956	NCGC00185097-01	$N(CH(CH_3)_2$	16 [14], n = 2
38	46925886	99430957	NCGC00185099-01	NH	18 [7], n = 2

Table 2. SAR Table - APE1 inhibition: representative analogs. Note: all compounds in table were synthesized at NCGC. ND = not determined. * low maximum response in HTS.

3.5 Cellular Activity

Cytotoxicity Studies (MTT Assay) of ML199:

- HeLa cells: % viability- (98% @ 5 µM), (79% @ 20 µM), (~5% @ 50 µM)
- T98G cells: % viability- (99% @ 5 µM), (95% @ 20 µM), (~80% @ 50 µM)
- U-87 MG cells: % viability- (35% @ 5 µM), (20% @ 20 µM), (~20% @ 50 µM)
- U-138 MG cells: (92% @ 5 µM), (80% @ 20 µM), (~50% @ 50 µM)
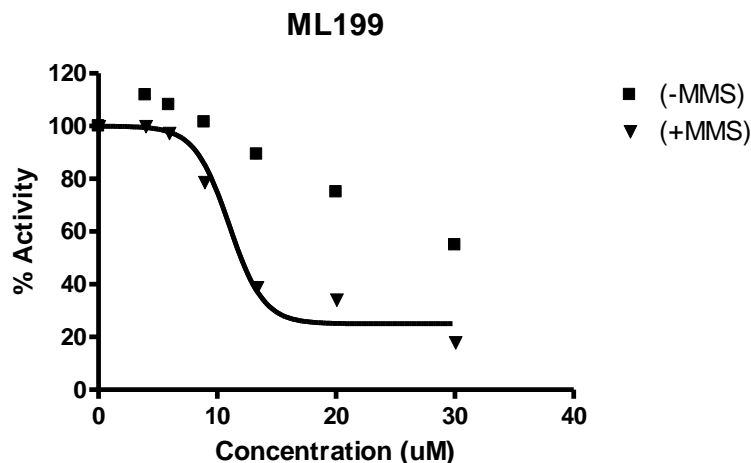
MMS Potentiation:

Figure 5. Potentiation of probe ML199 in the presence or absence of MMS.

3.6 Profiling Assays

ADME profiling:

Compound	Aq. Kinetic Sol. (PBS @ pH 7.4)	CYP2D6 (Inh. @ 10 μM)	CYP34A (Inh. @ 10 μM)	Caco-2 (P_{app} 10^{-6} m/s @ pH 7.4)	Efflux Ratio (B→A)/ (A→B)	hERG Inhibition (IC_{50}) Patch Clamp	Mouse Liver Microsome Stability (T1/2)	PBS-pH 7.4 Stability: % remaining after 48hrs	Mouse Plasma Stability (T1/2)
34*	51.6	39%	50%	6.8	0.8	8 μM	7.8 min.	100%	213 min.
1	20.4	0%	53%	5	1.1	0.7 μM	80 min.	100%	∞

Table 3. *In vitro* ADME to date. Green = desirable property, Yellow = less than desirable property, Red = undesirable property. All experiments were conducted by Shanghai Chempartner Co. Ltd. * indicates probe molecule (*see* Table 2).

As shown in the **Table 3**, both compound **1** (CID 3581333) and the probe molecule **34** (ML199, *see* **Table 2**) have many favorable attributes, yet a few liabilities exist. Compound **34** was chosen as the probe molecule because of its greatly improved potency in the secondary radiotracer assay (1 μM for **34** vs. 19 μM for **1**). The probe molecule also exhibits improved kinetic solubility, Caco-2 permeability and 10-fold less inhibition of the hERG channel or the HTS "hit" compound. Though the probe molecule is susceptible to mouse liver microsomes, compound **1** shows favorable stability. This seems to indicate that the general core scaffold is metabolically stable, and through additional structural modifications, this potential liability of the probe molecule could be addressed while maintaining potency.

No additional profiling studies have been conducted on the probe compound. This novel probe does not have any additional data in literature or in PubChem.

4 Discussion

Our initial SAR investigations involved modification of the piperidine nitrogen moiety (see entries **1-6** in **Table 1**). Changes to this position were well tolerated except for the introduction of the Boc-group (entry **3**), which resulted in a 3-fold loss of activity. Removal of the isopropyl group (R_3 = H, entry **2**) led to an increase in potency [IC_{50} = 6 μM (HTS assay) and 5 μM (RIA)]. Consequently, many of the subsequent analogs were synthesized without the isopropyl group, which saved one synthetic step.

The next area of SAR exploration involved modification of the benzothiazole moiety at the 3-position of the thiophene. As shown in the SAR Table above, many of the changes were not well tolerated; however, select modifications maintained activity of the parent compound. Removal of the benzothiazole (R_2 = H, entry **7**) resulted in essentially complete loss in activity. Other heterocycles were synthesized (entries **8**-**12**, **14-15**); however, only the 2-(4-phenylthiazole) analog (**15**) displayed potent inhibition. Interestingly, several simple phenyl substituted analogs (entry **13**) and other differentially substituted phenyl ring analogs (data not shown), failed to show even moderate inhibition of APE1. These results suggest that the thiazole moiety (or analogous heterocycle) is involved in an essential interaction in the APE1 binding site and should be maintained in some capacity in future analogs. Given that entry **15** had comparable potency to the requisite benzothiazole moiety, a phenyl ring scan of the pendant aryl ring may prove fruitful.

The goal of entries **16-29** was to gain a better understanding of the SAR associated with the N-acetyl moiety of the lead compound **1**. As such, a variety of different analogs were prepared, including numerous amides, carbamates, des-acetyl, carboxylic acids, esters, and amide bioisosteres (1,2,4-oxadiazoles and 1,3,4-oxadiazoles). Our first interest was to look at the des-acetyl analog (entry **29**); as shown in the above SAR Table, this modification was clearly unfavorable, with a 4-fold loss in activity. Many of the amide analogs resulted in a decrease in potency (e.g. *t*-Butyl (**16**) = 25 μM, cyclopropane (**17**) = 18 μM, CF_3 (**20**) = 31 μM). However, other amide analogs exhibited comparable if not improved potency (e.g. homo-propargyl (**24**) =

11 µM, CHF$_2$ (**22**) = 3 µM, and cyclopentane (**18**) = 11 µM). Replacing the amide with other functional groups, such as a carboxylic acid or ester, resulted in a dramatic loss of potency (data not shown); however, methylcarbamate (**21**) showed a 2-3-fold improvement in activity over compound **1**. We were also eager to explore the tolerance of amide bioisosteres, such as 1,2,4-oxadiazoles and 1,3,4-oxadiazoles. Toward this end, both analogs that lacked the 2-amino group (**25** and **26**) and those that maintained this moiety (**27** and **28**) were investigated. Interestingly, both the 1,3,4-oxadiazole (**27**) and 1,2,4-oxadiazole analog (**28**) showed comparable activity to the lead compound **1** (16 µM vs. 10 µM), providing the possibility of utilizing such modifications if necessary, based on future pharmacokinetic studies on this class of compounds.

Having explored the various functional groups around the core of the molecule, we then aimed to investigate modifications to the piperidine ring. As shown in **Tables 1** and **2**, most of these changes we met with limited success; however, a few interesting lessons were learned. Replacing the nitrogen with oxygen (entry **30**) or sulfur (entry **31**) had a moderate effect on potency, with IC$_{50}$ values of 18 and 16 µM, respectively. Sulfone derivative **32** (low max response in HTS) and pyridine analog (data not shown) both resulted in a loss of activity. Next, we explored various ring sizes and found that pyrrolidine analogs **34** and **35** displayed 19-fold and 5-fold improvement in potency, respectively, over compound **1** in the radiotracer assay (RIA). In the HTS assay, both compounds had comparable potency; however, the radiotracer incision assay results are considered the "golden standard" for final IC$_{50}$ determination. It should be noted that this assay is more laborious and very low throughput, so only select compounds are profiled in this system. Differentially substituted piperidine analog **33** displayed lower potency (45 µM); however, the seven-membered ring analogs **36-38** maintained comparable activity to **1**.

Compound **34** (ML199) exhibited good potency in the secondary radiotracer assay and gave a favorable ADME profile (see Section 3.6). Furthermore, ML199 was shown to potentiate the toxicity of DNA-damaging agent MMS in a subsequent cell-based assay (**Figure 5**) while exhibiting only moderate cytotoxicity with the probe compound alone. Mechanism of action of the probe and the original hit were explored, and both compounds were shown to act as competitive inhibitors of APE1 (**Figure 6**). An electrophoretic mobility shift assay (EMSA), was employed to examine the stability of the APE1-DNA substrate complex in the presence of ML199 (**Figure 7**). The percent APE1-DNA complex decreased with the increasing

concentration of the probe compound, further supporting the notion that ML199 acts by competitive inhibition and binds to Ape1 at the same site as the DNA substrate. On target effect of the probe was explored using HeLa whole cell extract incision assay in which ML199 was shown to inhibit AP Site incision activity which comparable activity as the purified enzyme assay (**Figure 8**).

SAR Summary:
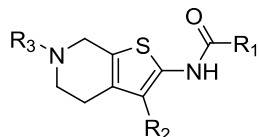
R_1 = various groups are tolerated here.   (e.g. Me, CHF_2, OMe, homopropargyl, amide bioisosteres)

R_2 = tight SAR, benzothiazole (and thiazole analogs) preferred. Simple replacement with phenyl group results in complete loss in activity. Removal of benzothiazole also kills activity.

R_3 = (ordered in decreasing potency) H ~ Me > Ac ~ isopropyl > Bn > Boc

Piperidine ring changes: (ordered in decreasing potency) pyrrolidine > piperidine ~ azepane > tetrahydropyran ~ tetrahydrothiopyran > differentially substituted piperidine > pyridine
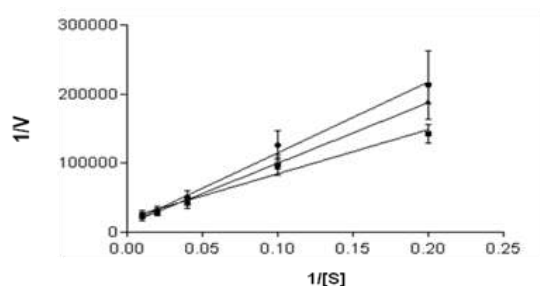
4.1   Comparison to existing art and how the new probe is an improvement

ML199 is more selective inhibitor of APE1 when compared to Compounds **1-4**. It is an ideal starting point for further development of the probe as a pre-clinical lead for drug discovery.

4.2   Mechanism of Action Studies

**Enzyme Kinetic Studies**

Mode of Inhibition: **Competitive**

	K_M (nM)	k_{cat} (min^{-1})	k_{cat}/K_M
No Inhibitor (■)	31.5	175	3.7
ML199 (●)	81.1	282	2.3
Compound **1** (▲)	70.2	285	2.7

Figure 6. Kinetic parameters without and with ML199 or Compound **1**. Ten pg of APE1 (~28 pM) was incubated without or with 5 μM of the indicated inhibitor at room temperature for 15 min. Increasing concentrations of radiolabeled abasic DNA substrate (i.e. 5, 10, 25, 50, or 100 nM) were then added, and the reactions were incubated at 37 ℃ for 5 min before the addition of stop buffer. Intact substrate was separated from incised product on a 15% polyacrylamide denaturing gel, and the percent conversion was determined by standard phosphorimager analysis. Lineweaver – Burk plots of 1/V versus 1/[S] were used to determine K_M and k_{cat} (shown). The plotted data points (averages and standard deviations) were derived from 11 independent values for the no inhibitor reactions, and 5 values for each of the inhibitor points.

Interference of APE1-DNA Complex Formation
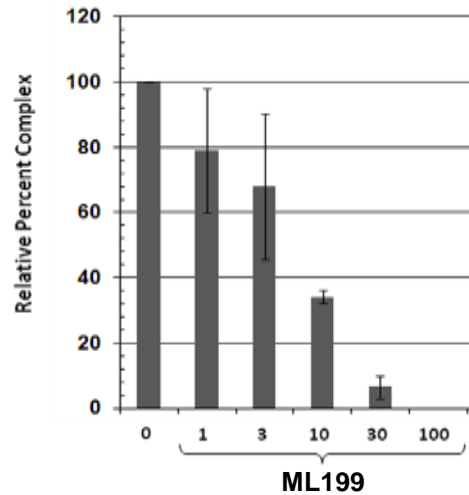
A
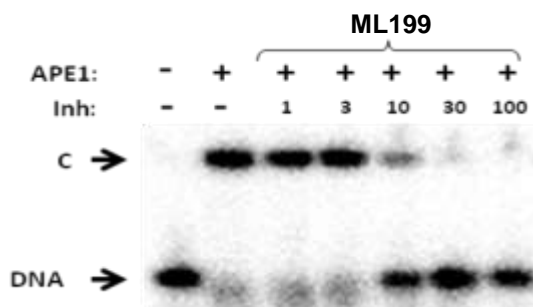
B

Figure 7. Stability of the APE1-DNA substrate complex in the presence of ML199. (**A**) Representative EMSA. Three hundred ng of APE1 (~0.8 μM) was incubated without inhibitor (final concentration 1% DMSO) or with the indicated inhibitor (1, 3, 10, 30 or 100 μM) for 10 min on ice. One hundred fmol of abasic DNA substrate (10 nM) was then added, and the binding reaction was incubated on ice for an additional 5 min. At that time, samples were subjected to non-denaturing polyacrylamide gel electrophoresis to separate the APE1-DNA complex (C) from unbound radiolabeled DNA (DNA). Inh = inhibitor. (**B**) Relative complex formation without ("0") or with the indicated inhibitor (in μM). Shown is the average and standard deviation of three independent experimental data points, all relative to the APE1 control, without inhibitor.

Inhibition of AP Site Incision Activity of Whole Cell HeLa Extracts.
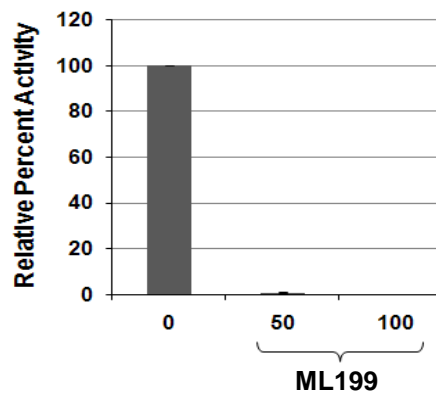

Figure 8. Inhibition of HeLa whole cell extract AP site incision activity with ML199. Three hundred ng of HeLa whole cell extract was incubated with 0, 50 or 100 μM of the indicated inhibitor at room temperature for 15 min, prior to the addition of 0.5 pmol radiolabeled AP-DNA substrate and subsequent transfer of the reaction mix (final volume of 10 μL) to 37 °C for 5 min to allow for incision. Following addition of stop buffer and heat denaturation, the reaction products were subjected to 15% polyacrylamide denaturing gel electrophoresis. Shown is a bar graph reporting the relative percent incision activity in comparison to the no inhibitor control, arbitrarily set at 100. The values reported represent the averages and standard deviation of three independent experimental data points.

4.3   Planned Future Studies

Future studies of this probe molecule include submitting the probe and related analogs to the NCI-60 panel, analysis of the pharmacokinetics (mouse species), and additional pre-clinical experiments, such as Xenograft studies (primarily as a combination therapy with known DNA damaging cancer chemotherapeutics such as TMZ). Additional planned experiments include TMZ potentiation with U-87 glioma line, AP site accumulation studies and isothermal titration calorimetry (ITC) characterization. We plan to submit an extended probe characterization proposal to provide the funds to carry out such studies.

5   References

[1] Wilson, D.M., III and Bohr, V.A. (2007) The mechanics of base excision repair, and its relationship to aging and disease. *DNA Repair (Amst)*, 6, 544-559.

[2] Wilson, D.M., III and Barsky, D. (2001) The major human abasic endonuclease: formation, consequences and repair of abasic lesions in DNA. *Mutat. Res.*, 485, 283-307.

[3] Demple, B. and Sung, J.S. (2005) Molecular and biological roles of APE1 protein in mammalian base excision repair. *DNA Repair (Amst)*, 4, 1442-1449.

[4] Xanthoudakis, S., Smeyne, R.J., Wallace, J.D. and Curran, T. (1996) The redox/DNA repair protein, Ref-1, is essential for early embryonic development in mice. *Proc. Natl. Acad. Sci. U. S. A,* 93, 8919-8923.

[5] Fung, H. and Demple, B. (2005) A vital role for ape1/ref1 protein in repairing spontaneous DNA damage in human cells. *Mol. Cell*, 17, 463-470.

[6] Izumi, T., Brown, D.B., Naidu, C.V., Bhakat, K.K., MacInnes, M.A., Saito, H., Chen, D.J. and Mitra, S. (2005) Two essential but distinct functions of the mammalian abasic endonuclease. *Proc. Natl. Acad. Sci. U. S. A*, 102, 5739-5743.

[7] Fishel, M.L. and Kelley, M.R. (2007) The DNA base excision repair protein APE1/Ref-1 as a therapeutic and chemopreventive target. *Mol. Aspects Med.*, 28, 375-395.

[8] McNeill, D.R. and Wilson, D.M., III (2007) A dominant-negative form of the major human abasic endonuclease enhances cellular sensitivity to laboratory and clinical DNA-damaging agents. *Mol. Cancer Res.*, 5, 61-70.

[9] Lieberman, H.B. (2008) DNA damage repair and response proteins as targets for cancer therapy. *Curr. Med. Chem.*, 15, 360-367.

[10] Zaremba, T. and Curtin, N.J. (2007) PARP inhibitor development for systemic cancer targeting. *Anticancer Agents Med. Chem.*, 7, 515-523.

[11] Horton, J.K. and Wilson, S.H. (2007) Hypersensitivity phenotypes associated with genetic and synthetic inhibitor-induced base excision repair deficiency. *DNA Repair (Amst)*, 6, 530-543.

[12] Wyatt, M.D. and Pittman, D.L. (2006) Methylating agents and DNA repair responses: Methylated bases and sources of strand breaks. *Chem. Res. Toxicol.,* 19, 1580-1594.

[13] Mutter, N. and Stupp, R. (2006) Temozolomide: a milestone in neuro-oncology and beyond? Expert. Rev. *Anticancer Ther.,* 6, 1187-1204.

[14] Longley, D.B., Harkin, D.P. and Johnston, P.G. (2003) 5-fluorouracil: mechanisms of action and clinical strategies. *Nat. Rev. Cancer,* 3, 330-338.

[15] An, Q., Robins, P., Lindahl, T. and Barnes, D.E. (2007) 5-Fluorouracil incorporated into DNA is excised by the Smug1 DNA glycosylase to reduce drug cytotoxicity. *Cancer Res.*, 67, 940-945.

[16] Madhusudan, S.; Smart, F.; Shrimpton, P.; Parsons, J. L.; Gardiner, L.; Houlbrook, S.; Talbot, D.; Hammonds, T.; Freemont, P. A.; Sternberg, M. J. E.; Dianov, G. L.; Hickson, I. D. Isolation of a small molecule inhibitor of DNA base excision repair. *Nucleic Acids Res.* 2005**,** *33*, 4711-4724.

[17] Seiple, L. A.; Cardellina 2nd, J. H.; Akee, R.; Stivers, J. T. Potent inhibition of human apurinic/apyrimidinic endonuclease 1 by arylstilbonic acids. *Mol. Pharmacol.* 2008, *73*, 669-677.

[18] Zawahir, Z.; Dayam, R.; Deng, J.; Pereira, C.; Neamati, N. Pharmacophore guided discovery of small-molecule human apurinic/apyrimidinic endonuclease APE1. *J. Med. Chem.* 2009, *52*, 20-32.

[19] Bapat, A.; Glass, L. S.; Luo, M.; Fishel, M. L.; Long, E. C.; Georgiadis, M. M.; Kelley, M. R. Novel small molecule inhibitor of APE1 endonuclease blocks proliferation and reduces viability of glioblastoma cells. *J. Pharmacol. Exp. Ther.* 2010, 334, 988-998.

[20] Simeonov, A.; Kulkarni, A.; Dorjsuren, D.; Jadhav, A.; Shen, M.; McNeill, D. R.; Austin, C. P. Wilson, D. M. III. Identification and characterization of inhibitors of human apurinic/apyrimidinic endonuclease APE1. *PLos ONE*, 2009, *4*, e5740.

[21] Tse W, Boger DL. (2004) A Fluorescent Intercalator Displacement Assay for Establishing DNA Binding Selectivity and Affinity. *Acc Chem Res.* 37(1):61-9.

[22] Erzberger, J. P.; Barsky, D.; Scharer, O. D.; Colvin, M. E.; Wilson, D. M. III Elements in abasic site recognition by the major human and Escherichia coli apurinic/apyrimidinic endonucleases. *Nucleic Acids Res.* 1998, 26, 2771-2778.

[23] Wilson, D. M., III; Takeshita, M.; Grollman, A. P.; Demple, B. Incision activity of human apurinic endonuclease (Ape) at abasic site analogs in DNA. *J. Biol. Chem.* 1995, 270, 16002-16007.

[24] Wilson, D. M., III; Takeshita, M.; Demple, B. Abasic site binding by the human apurinic endonuclease, Ape, and determination of the DNA contact sites. *Nucleic Acids Res.* 1997, 25, 933-939.

[25] Gewald, K.; Schinke, E.; Bo¨ttcher, H. 2-Amino-thiophene aus methylenaktiven Nitrile carbonylverbindiungen und Schwefel. *Chem. Ber*. 1966, *99*, 94-100.

[26] Andersen, H. S.; Olsen, O. H.; Iversen, L. F.; Sorensen, A. L. P.; Mortensen, S. B.; Christensen, M. S.; Branner, S. ; Hansen, T. ; Lau, J. F.; Jeppesen, L.; Moran, E. J.; Su, J.; Bakir, F.; Judge, L.; Shahbaz, M.; Collins, T.; Vo, T.; newman, M. J.; Ripka, W. C.; Moller, N. P. H. Discovery and SAR of a Novel Selective and Orally Bioavailable Nonpeptide Classical Competitive Inhibitor Class of Protein-Tyrosine Phosphatase 1B. *J . Med. Chem.* 2002, *45*, 4443-4459.